

Current GCMs' Unrealistic Negative Feedback in the Arctic

JULIEN BOÉ, ALEX HALL, AND XIN QU

Department of Atmospheric and Oceanic Sciences, University of California, Los Angeles, Los Angeles, California

(Manuscript received 7 October 2008, in final form 13 March 2009)

ABSTRACT

The large spread of the response to anthropogenic forcing simulated by state-of-the-art climate models in the Arctic is investigated. A feedback analysis framework specific to the Arctic is developed to address this issue. The feedback analysis shows that a large part of the spread of Arctic climate change is explained by the longwave feedback parameter. The large spread of the negative longwave feedback parameter is in turn mainly due to variations in temperature feedback. The vertical temperature structure of the atmosphere in the Arctic, characterized by a surface inversion during wintertime, exerts a strong control on the temperature feedback and consequently on simulated Arctic climate change. Most current climate models likely overestimate the climatological strength of the inversion, leading to excessive negative longwave feedback. The authors conclude that the models' near-equilibrium response to anthropogenic forcing is generally too small.

1. Introduction

The Arctic has become emblematic of climate change, given the spectacular changes observed over recent decades and expected to occur during the next century in response to anthropogenic forcing. While global mean surface temperature has increased about 0.7 K since the beginning of the twentieth century, Arctic temperature has increased at twice that rate (Solomon et al. 2007). State-of-the-art climate simulations carried out in the context of the Intergovernmental Panel on Climate Change Fourth Assessment Report (IPCC AR4) have confirmed that surface warming in response to anthropogenic forcing will be greatly amplified in the Arctic (Meehl et al. 2007a). A major reduction of sea ice cover during summer is also expected, with a possibility that ice-free conditions in September become the norm before the end of the twenty-first century (Holland et al. 2006).

In this context, Arctic climate is monitored carefully. It is difficult to prove that the exceptional sea ice decline of 2007 (Zhang et al. 2008) is linked to anthropogenic climate change, as it is always difficult to determine whether an extreme event with such a short time scale is

due to the steady increase in radiative forcing since the beginning of the industrial era (Hegerl et al. 2007). However, it is clear that global change increases the likelihood of such an event. Moreover, the exceptional sea ice decline of 2007 occurs following several decades characterized by a large decreasing trend in September sea ice extent (Serreze et al. 2007). The fact that current climate models show a smaller decline in sea ice cover than observed (Stroeve et al. 2007) is intriguing and worrying, and it suggests climate models might also underestimate future climate change in the Arctic.

If some features of Arctic climate change are now well established, major uncertainties remain. Indeed, the spread among the temperature change of the current climate models is greatest in the Arctic. These uncertainties are not merely a local issue given the key role of the Arctic in the earth's climate. In this context, a better understanding of the physical mechanisms governing simulated Arctic climate change and its uncertainties is needed. The role of snow and sea ice in Arctic climate change has long been recognized (Budyko 1969; Sellers 1969; Robock 1985; Holland and Bitz 2003; Hall 2004). Given their high reflectivity to sunlight, the reduction of snow or sea ice cover initiated by anthropogenic forcing leads to an increase of absorbed shortwave radiation, inducing a further increase of temperature. This specific sea ice–snow albedo positive feedback (Curry et al. 1995) is generally considered to play a key role in so-called Arctic amplification. But even if sea ice–snow

Corresponding author address: Julien Boé, Department of Atmospheric and Oceanic Sciences, University of California, Los Angeles, Los Angeles, CA 90095.
E-mail: boe@atmos.ucla.edu

albedo feedback plays a key role in the ensemble-mean response to anthropogenic forcing, this feedback may not necessarily be the main factor behind the model-to-model differences. Indeed, other mechanisms, such as atmospheric circulation changes (Cai 2006), oceanic circulation changes (Holland and Bitz 2003), or short-wave feedback unrelated to the sea ice–snow albedo feedback (Winton 2006) have also been proposed as potential contributors to the spread of the simulated Arctic amplification.

To determine which physical mechanisms contribute most to the spread in simulated Arctic climate change, we develop a feedback analysis framework taking into account the peculiarities of Arctic climate change. Our study is based on analysis of an ensemble of state-of-the-art climate simulations carried out in conjunction with the IPCC AR4. We begin with a reexamination of the notion of Arctic amplification and an analysis of the basic features of simulated Arctic climate change (section 2). This lays the groundwork for a feedback analysis framework specific to the Arctic (section 3). The analysis of an ensemble of climate simulations using this framework leads to the conclusion that the longwave feedback parameter, generally overlooked, is a crucial factor behind the spread in Arctic climate response (section 4). We then explain the spread of the longwave feedback parameter and we show that the temperature feedback plays a major role (section 5). The climatological inversion of the temperature profile near the surface in the Arctic is especially important in controlling the magnitude of water vapor and temperature feedbacks. Moreover, the magnitude of the temperature feedback is linked to the climatological value of the inversion simulated by the climate models (section 6). As current climate models seem to overestimate the strength of the inversion, we suspect they underestimate climate change in the Arctic (section 7). Finally, the main conclusions are summarized in section 8.

2. Basic features of simulated Arctic climate change

The dominant features of Arctic climate change have been highlighted by previous studies. The most important are probably the large amplification of the surface warming (Holland and Bitz 2003) and the large seasonal redistribution of energy within the climate system in the Arctic region (Manabe and Stouffer 1980). In this first section, we determine whether these classic features of Arctic climate change hold for the state-of-the-art coupled atmospheric–oceanic general circulation models from the World Climate Research Programme’s Coupled Model Intercomparison Project phase 3 (CMIP3) multimodel dataset (Meehl et al. 2007b) carried out in

the context of the IPCC AR4. As we are interested in as near an equilibrium climate as possible given our dataset, we analyze the climate simulations forced by the Special Report on Emissions Scenarios (SRES) A1B scenario, for which the anthropogenic forcing is kept constant after 2100. The reference climatological means are computed over the 1900–49 period of the twentieth-century simulations (20C3M) and the period used to compute the climatological anomalies is 2150–99. We do not use data from beyond this period because too few simulations are available for the twenty-third century. Given the availability of the data necessary for our study, mainly 13 models are studied. They are the Canadian Centre for Climate Modelling and Analysis (CCCma) Coupled General Circulation Model, version 3.1 (CGCM3.1); CCCma CGCM3.1 T63; Centre National de Recherches Météorologiques Coupled Global Climate Model, version 3 (CNRM-CM3); Commonwealth Scientific and Industrial Research Organisation Mark version 3.0 (CSIRO Mk3.0); Geophysical Fluid Dynamics Laboratory Climate Model version 2.0 (GFDL CM2.0); GFDL CM2.1; Goddard Institute for Space Studies Model E-R (GISS-ER); L’Institut Pierre-Simon Laplace Coupled Model, version 4 (IPSL CM4); Model for Interdisciplinary Research on Climate 3.2, medium-resolution version [MIROC3.2(medres)]; ECHAM and the global Hamburg Ocean Primitive Equation (ECHO-G); Meteorological Research Institute Coupled General Circulation Model, version 2.3.2a (MRI CGCM2.3.2a); National Center for Atmospheric Research (NCAR) Parallel Climate Model version 1 (PCM1); third climate configuration of the Met Office Unified Model (UKMO HadCM3). Note that these models cannot be considered fully independent because some of them share identical components or physical parameterizations and may not span the full range of uncertainty surrounding climate change (Tebaldi and Knutti 2007). In this paper, the Arctic is defined as the region where latitude is greater than 70°N, and all the diagnostics are computed for this domain.

First of all, the notion of “Arctic amplification” is reexamined. This term generally refers to the larger increase of surface temperature (T_{as}) in the Arctic compared to the rest of the world (Holland and Bitz 2003). The zonal mean T_{as} change over the oceans (black curve in Fig. 1) illustrates the notion of Arctic amplification. The warming in the Arctic is roughly 3 times greater than that of the tropics and midlatitudes. The intermodel spread in the Arctic is also greater.

A different picture emerges when we look at the change in the heat content of the oceanic mixed layer–atmosphere system. Here, heat content change is calculated as the sum of the change in the internal heat of seawater within the mixed layer and the amount of heat

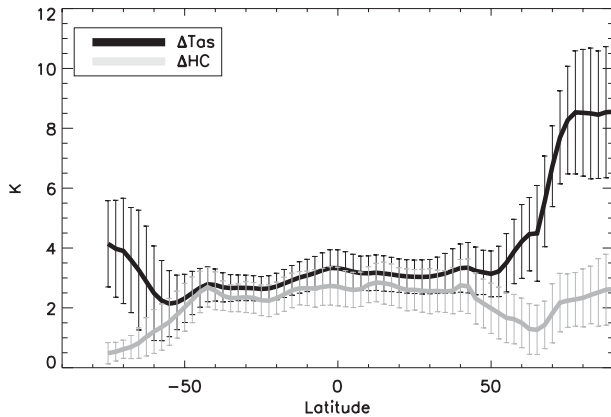


FIG. 1. Annual zonal mean change of surface temperature (T_{as} , K) over oceans and of heat content of the oceanic mixed layer-atmosphere system expressed as a change of temperature within the uppermost 70 m of ocean (HC, K) (see text for the calculation of the heat content) at the end of the twenty-second century. The lines stand for the ensemble means and the bars stand for the intermodel spread measured by one std dev.

corresponding to sea ice melting between the present and future climate. The heat content of the atmosphere is neglected because of the relatively low heat capacity of the air. The value of heat content change is then expressed as a change of temperature within the mixed layer:

$$\Delta HC = \frac{(\rho_w c_p \Delta T_{oc} V + \rho_i L_i \Delta V_i)}{\rho_w c_p V}, \quad (1)$$

where ΔHC is the change of heat content, ρ_w and ρ_i are the density of seawater and ice, c_p is the heat capacity of seawater, V is the volume of the mixed layer, L_i is the latent heat of melting of ice, ΔV_i is the change in ice volume, and ΔT_{oc} is the mean change in oceanic temperature in the mixed layer. As the effective heat capacity of continental surface is small compared to that of ocean, and, moreover, as our study area is largely oceanic, the value given by Eq. (1) is representative of the heat content change in the whole study area. We define the mixed layer as the uppermost 70 m of ocean, because 70 m is a value representative of the Arctic (de Boyer Montégut et al. 2004). Note that the results of this study are not sensitive to the precise definition of the mixed layer depth.

The gray curve in Fig. 1 represents the zonal mean change of ΔHC . In contrast with T_{as} change, there is no amplification of heat content change in the Arctic. This point has important implications for our understanding of Arctic climate change. Generally, Arctic amplification is attributed to sea ice-snow albedo feedback. However, if Arctic amplification were directly linked to excess positive radiative feedback compared to other

regions, or indeed any process increasing the net energy of the region more than elsewhere, there should also be an amplification of heat content change. This raises the question of why is there no Arctic amplification of heat content increase despite the existence of a well-known strong positive radiative feedback in the region. An immediate hypothesis is that a large negative radiative feedback also plays an important role in the Arctic. A feedback analysis is needed to address this issue quantitatively.

Two more points are worth noting. First, we focus here on the mixed layer because we are mainly interested by the part of the ocean that is directly coupled to the atmosphere. But similar conclusions would be drawn if we considered the entire ocean; indeed, Fig. 10.7 of Meehl et al. (2007a) shows that there is also no Arctic amplification of oceanic temperature even considering the total column. Second, the fact that an especially large increase of surface atmospheric temperature occurs in the Arctic without a correspondingly large increase of heat content indicates that internal redistribution of energy among the different components of the Arctic climate system plays an important role in Arctic amplification. The energy redistribution may be facilitated by a decrease of the insulation effect of sea ice in the future climate. This is a well-known feature of Arctic climate change and leads to an increase of energy transfer from the ocean to the atmosphere (Manabe and Stouffer 1980; Robock 1985; Hall 2004).

The contrast in the behavior of T_{as} and heat content not only exists in annual mean change but it is also reflected in the seasonal changes of these variables, as shown in Fig. 2. This figure depicts the annual and seasonal changes of T_{as} and energy budget at the top of atmosphere (TOA) as well as the monthly change in the two components of heat content [see Eq. (1)]—gray bar: ΔT_{oc} , white bar: $(\rho_i L_i \Delta V_i) / (\rho_w c_p V)$. The change of T_{as} (Fig. 2b) is minimal during summer, while the net change of energy at the TOA is strongly positive because of a large positive anomaly of shortwave radiation (Fig. 2a). Conversely, during winter and autumn, the change of T_{as} is very large while the anomaly of the energy budget at the TOA is strongly negative because of a large increase of outgoing longwave radiation (OLR). This figure depicts the same basic features described by pioneering climate change studies such as Manabe and Stouffer (1980), with the well-known out-of-phase relation between the seasonal changes of T_{as} and of the radiative fluxes at the TOA. Figure 2c shows that T_{oc} is the main factor responsible for the seasonal variation of the changes of heat content.

Note that the sea ice albedo feedback is nearly inoperative during winter because incoming shortwave radiation

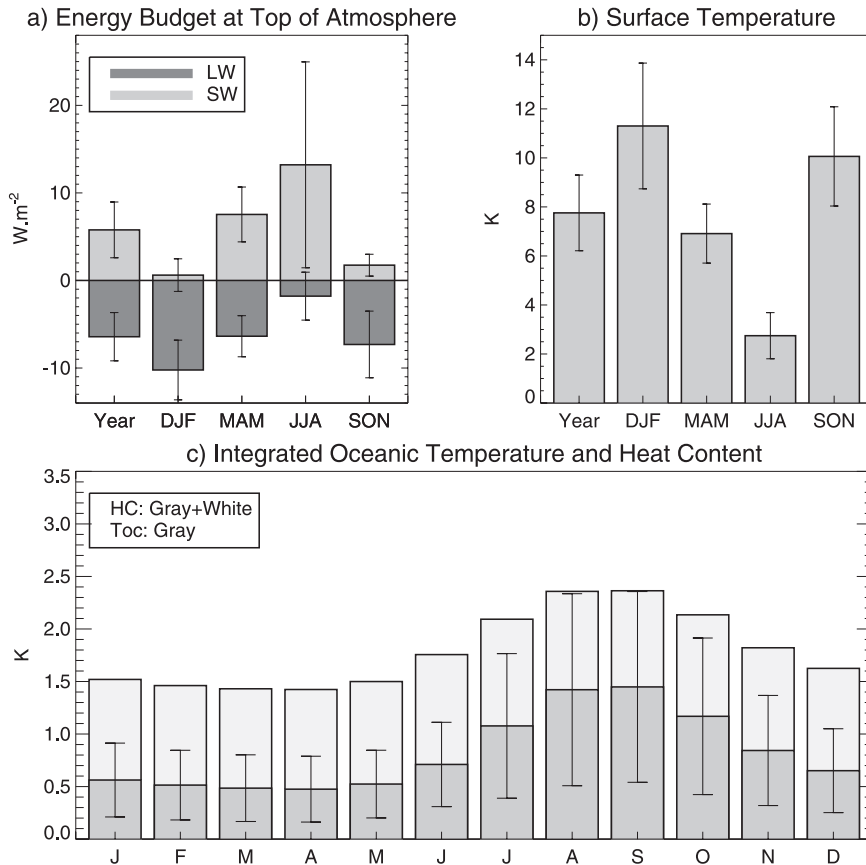


FIG. 2. Seasonal and annual change of (a) the energy budget at the top of atmosphere [net longwave radiation (LW); net shortwave radiation (SW)] and (b) surface temperature. (c) Monthly change of heat content of the oceanic mixed layer–atmosphere system expressed as a change of temperature within the uppermost 70 m of ocean and integrated oceanic temperature defined as averaged potential temperature in the uppermost 70 m of ocean in the Arctic. The large bars stand for the ensemble mean and the thin bars stand for the intermodel spread measured by one std dev.

is very weak in the Arctic. Therefore, this feedback cannot be directly responsible for the Arctic amplification of surface temperature that occurs mainly in winter. Its role is indirect: thanks to the sea ice albedo feedback in spring and summer, the ice cover decreases and solar energy is stored in the ocean; ΔT_{oc} progressively increases from April to September. In winter and fall, thinning sea ice and decreasing sea ice cover and their associated insulation effects lead to an increase of heat transfer from the ocean to the atmosphere and consequently to an increase in surface temperature (Manabe and Stouffer 1980; Robock 1985; Hall 2004). Given the stratification of the atmosphere during late autumn and winter in the Arctic, the resulting warming is trapped near the surface, which leads to a very large increase of T_{as} . The solar energy stored in the ocean during spring and summer is finally radiated to space as longwave radiation in autumn and winter. This damping prevents

some of the heat gained during summer from being carried through fall and winter. It plays a crucial role in limiting the increase of oceanic temperature and consequently Arctic climate change. The Arctic is therefore characterized not only by a strong positive feedback in summer but also by a strong negative longwave feedback that operates mainly in fall and winter.

In contrast with midlatitudes and tropics (not shown), Arctic climate change involves a large seasonal redistribution of energy within the climate system, with the ocean acting as a heat reservoir. The large increase of T_{as} in this region is largely the result of this redistribution of energy. The T_{as} does not respond directly to the change of the energy budget at the TOA but is essentially a by-product of the increase of summertime heat content and the reduction of winter sea ice. Though this point is not a new one, it is important to confirm that the latest models behave as previous generation of models,

since these well-known peculiarities of Arctic climate change have important implications for the development of a feedback analysis framework, as explained in the next section.

3. Feedback analysis framework

The climate response to anthropogenic forcing depends on the forcing's direct effect on the energy budget at the TOA and on how this initial perturbation is dampened or amplified by climate feedbacks, in particular radiative feedbacks. Generally, the longwave and shortwave feedback parameters, λ_{LW} and λ_{SW} , respectively, are defined as follows: $\lambda_{LW} = \Delta F / \Delta T_{as}$ and $\lambda_{SW} = \Delta Q / \Delta T_{as}$, where ΔT_{as} is the change of surface temperature, ΔQ is the change of net shortwave radiation at the TOA, ΔF is the change of longwave radiation at the TOA, the direct effect of the CO₂ forcing on OLR being removed. The value of the CO₂ forcing at CO₂ doubling is only given by six CMIP3 models. However, the intermodel spread of the CO₂ forcing among the six models in the Arctic is very small. Therefore, we used the same value for all the models studied in this paper. We computed the ensemble mean of the six models in the Arctic and then scaled logarithmically this value to obtain an estimate corresponding to the 720-ppm CO₂ concentration of the SRES A1B scenario (4.29 W m⁻² in the Arctic).

Generally, T_{as} is the right variable to use in the definition of the feedback parameters for analysis of climate change in the tropics and midlatitudes because it is representative of the change of the atmosphere–oceanic mixed layer system. However, if efficient heat fluxes across the air–sea interface are not possible, or if atmospheric convection does not exist to homogenize the atmosphere, T_{as} may not be the most representative and relevant metric of changes in the atmosphere–oceanic mixed layer system. In the Arctic, these conditions are often met: ice cover hampers an efficient coupling between ocean and atmosphere via surface heat fluxes, and the thermal inversion during winter prevents the homogenization of atmospheric changes. Surface temperature change is thus not a representative variable of the change in system's heat content in the Arctic as shown in Fig. 1. This is also consistent with the results of the previous section, namely that ΔT_{as} is mainly driven by the seasonal redistribution of energy and is essentially a by-product of the increase of oceanic temperature during summer and reduction in ice.

In this study, we propose to use ΔT_{oc} in the definition of the radiative feedback for the Arctic instead of ΔT_{as} because ΔT_{oc} is more representative of the thermal state of the atmosphere–oceanic mixed layer system. This is

consistent with the fact that oceanic temperature change directly responds to the change of the radiative fluxes at the TOA as shown in the previous section: it plays an active role in the reduction of sea ice cover and thickness and in the consequent increase of absorbed shortwave radiation. Therefore, the following definition of the feedback parameters in the Arctic is proposed:

$$\lambda_{LW} = \frac{\Delta F}{\Delta T_{oc}}, \quad (2)$$

$$\lambda_{SW} = \frac{\Delta Q}{\Delta T_{oc}}. \quad (3)$$

A feedback parameter is a mathematical concept intended to characterize and understand the response of the climate system to an external forcing. Therefore, the choice of a particular metric for the feedback parameters should be justified by its explanatory power. The explanatory power of the sum of the feedback parameters defined by Eqs. (2) and (3) for the change of T_{oc} is high, as a strong link between these two quantities is seen in Fig. 3a (correlation of 0.81). We chose ΔT_{oc} rather than ΔHC in the definition of the feedback parameters because the use of ΔHC leads to a weaker correlation of 0.60, despite the fact that ΔHC is a more complete measure of the change in system's heat content. Our explanation for this result is the dual role of the variable used to define the feedback parameters. First, it must correctly represent the change in the system's thermal state. Second, the TOA radiative fluxes determining feedback strength must be sensitive to it. The difference between ΔHC and ΔT_{oc} is simply the energy used to melt ice, proportional to ice volume change. There is no direct and simple relation between ice volume change and the radiative fluxes at the TOA. Apparently, TOA fluxes are most sensitive to the T_{oc} component of HC, as one might intuitively expect.

If the classical definition of the feedback parameters based on ΔT_{as} was adequate in the Arctic, one would expect a large part of the spread of ΔT_{as} to be explained by the sum of the feedback parameters. As shown in Fig. 3b, only a weak relation is visible between ΔT_{as} and the sum of the feedback parameters based on the classical definition, and the small correlation of 0.44 is not significant at the 0.05 level.

A more complete assessment of the power of the feedback parameters based on ΔT_{as} and ΔT_{oc} to explain various aspects of Arctic climate change is given in Table 1. This table shows that the definition of the feedback parameters based on Eqs. (2) and (3) is a better metric for all the aspects of Arctic climate change. Analysis of radiative feedback parameters based on this definition is

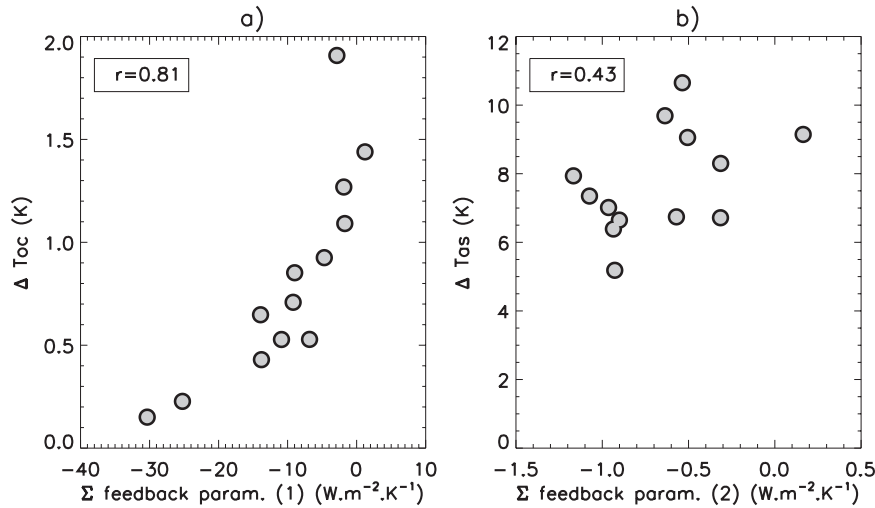


FIG. 3. Link between the sum of the longwave and shortwave feedback parameters and (a) T_{oc} when the feedback parameters are defined using T_{oc} and (b) T_{as} when the feedback parameters are classically defined using T_{as} . The value of the linear correlation coefficient is given on the graph. Note that for a sample of 13 values, the correlation corresponding to the 0.05 (0.01) significance level is 0.553 (0.684).

therefore a much improved starting point to understand Arctic climate change.

4. Identification of the key feedback

The next step is to determine the respective roles of the longwave and shortwave feedback parameters in the spread of oceanic temperature change in response to anthropogenic forcing. The correlation between ΔT_{oc} in the CMIP3 models and λ_{LW} is 0.78. Note that, by our convention, λ_{LW} is negative, and a large absolute value indicates a strong negative feedback. Therefore, models with larger oceanic temperature change have a smaller negative longwave feedback parameter and hence a weaker negative feedback. This value is very close to the correlation of 0.81 obtained previously between the sum of the feedback parameters and ΔT_{oc} (section 3), which suggests that λ_{LW} is the key factor of the spread of oceanic temperature change. By contrast, the correlation between ΔT_{oc} and λ_{SW} is much weaker (-0.51) and its sign is not the one physically expected. Indeed, a large value of λ_{SW} does not correspond to a large value of ΔT_{oc} . To understand this counterintuitive result, we note that the moderate negative correlation between λ_{SW} and ΔT_{oc} arises because the variations in λ_{SW} and λ_{LW} are themselves closely anticorrelated (correlation coefficient of -0.84). This occurs because both longwave and shortwave feedbacks are linked to the change in sea ice cover. A decrease of sea ice cover leads to an increase of absorbed radiation. But as ice cover has also a strong insulation effect and hampers the heat exchange be-

tween the ocean and the atmosphere, it also leads to an increase of wintertime surface air temperature and an increase of OLR. Thus, in a given climate model, λ_{SW} and λ_{LW} ought to be related through the sensitivity of sea ice cover change to oceanic warming: for a given ΔT_{oc} , the increase of absorbed shortwave radiation and the increase of OLR are both expected to be larger for a greater decrease of sea ice cover. To test this hypothesis, the correlation between λ_{SW} and $\Delta S_{ic}/\Delta T_{oc}$ and λ_{LW} and $\Delta S_{ic}/\Delta T_{oc}$ are computed, where S_{ic} is the sea ice extent. The high correlations obtained (-0.85 and 0.86 , respectively) confirm the hypothesis that λ_{SW} and λ_{LW} are strongly linked to one another through sea ice reduction. While the same process creates variations in λ_{LW} and λ_{SW} , which leads to the two components being anticorrelated, the variations in λ_{LW} are much larger than the variations in λ_{SW} (the spread of λ_{SW} measured as one standard deviation is 2 times smaller than the spread of λ_{LW} : $6.50 \text{ W m}^{-2} \text{ K}^{-1}$ versus $14.25 \text{ W m}^{-2} \text{ K}^{-1}$). So the reduction in sea ice is associated with larger anomaly in negative longwave feedback than positive shortwave feedback. The dominance of the negative longwave

TABLE 1. Correlation of the sum of the feedback parameters, defined classically using surface temperature change and using the definition given by Eqs. (2) and (3), with surface temperature change, oceanic temperature change, and change in sea ice extent (ΔS_{ic}).

	ΔT_{as}	ΔT_{oc}	ΔS_{ic}
Feedbacks defined using ΔT_{as}	0.44	0.62	-0.48
Feedbacks defined using ΔT_{oc}	0.60	0.81	-0.81

feedback and its link to sea ice reduction explains why smaller warming is paradoxically associated with larger positive shortwave feedback.

In this section, we have shown that the shortwave feedback parameter is not a determining factor in the spread of ΔT_{oc} and that the key role is played by the longwave feedback parameter. Though an important role for λ_{LW} was suggested by the fact that, despite the existence of the strong positive snow albedo feedback, there is no Arctic amplification of heat content increase (Fig. 1), this is a surprising result, as the role of λ_{LW} in the Arctic has generally been overlooked. The results shown in this section do not mean that sea ice–snow albedo feedback is not important for Arctic climate change. This feedback is indeed critical for the ensemble-mean response of the CMIP3 models to anthropogenic climate change and contributes significantly to positive feedback levels in the modeled Arctic and probably in the real Arctic as well; however, it does not play a dominant role in the intermodel spread.

5. Analysis of the spread of the longwave feedback parameter

The results of the previous section show that, to make progress in understanding the uncertainties of Arctic climate change, it is necessary to explain the intermodel spread of the longwave feedback parameter. The longwave feedback has mainly three components: temperature feedback, water vapor feedback, and longwave cloud cover feedback (Bony et al. 2006). In the classical approach of Wetherald and Manabe (1988), adapted to our framework, the longwave feedback parameter associated with variable X , λ_X , can be written as the product of two terms:

$$\lambda_X = \frac{\partial F}{\partial X} \frac{\Delta X}{\Delta T_{oc}}. \quad (4)$$

The longwave feedback parameter associated with a variable X depends on how the variable X changes in response to a given change of T_{oc} and also how the OLR changes in response to a variation of X , all the other climate variables being identical.

The total longwave feedback parameter can therefore be written as follows:

$$\lambda_{LW} = \sum_X \frac{\partial F}{\partial X} \frac{\Delta X}{\Delta T_{oc}}. \quad (5)$$

In this formula, X could be any climate variable, but the term $\partial F/\partial X$ will be different from zero for only temperature, cloud cover, and water vapor variables.

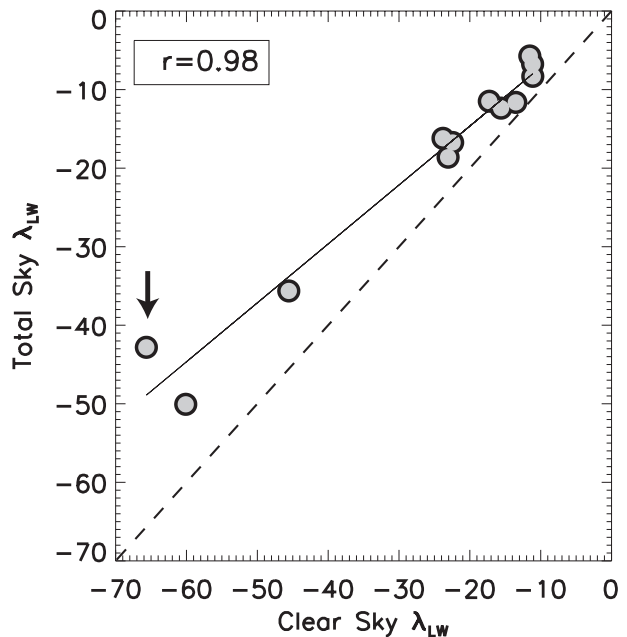


FIG. 4. Total-sky longwave feedback parameter vs clear-sky longwave feedback parameter ($\text{W m}^{-2} \text{K}^{-1}$). The plain line is the regression line. The dashed line stands for the equation $y = x$. The black arrow indicates the outlier shown in Fig. 7 and discussed in section 6. The correlation obtained when the three models with the most negative longwave feedback are excluded is 0.95.

Here, we assess the respective roles of the three components of the longwave feedback.

The role of longwave cloud feedback can be estimated by comparing the clear-sky longwave parameter and total-sky longwave feedback parameters previously estimated. The clear-sky longwave feedback parameter is estimated by substituting the OLR in Eq. (2) with the clear-sky OLR, an output of the CMIP3 models. Fig. 4 shows that most of the spread of the total-sky longwave feedback parameter is accounted for by the clear-sky feedback parameter (correlation coefficient of 0.98). The cloud feedback thus has almost no impact on the spread of the longwave feedback parameter. The longwave cloud feedback is positive in all the models, as the absolute value of the total-sky feedback parameter is smaller than the absolute value of the clear-sky feedback parameter. This is expected since the CMIP3 models simulate an increase of the cloud cover in the Arctic, mostly near the top of the tropopause (Meehl et al. 2007a). However, the longwave cloud feedback is small, as the deviation of the regression line in Fig. 4 from a diagonal (dashed line) is small compared to the absolute value of the total- or clear-sky longwave feedback parameter. Note that Soden et al. (2008) has shown that the total cloud feedback (including longwave and shortwave components) is negative in the Arctic,

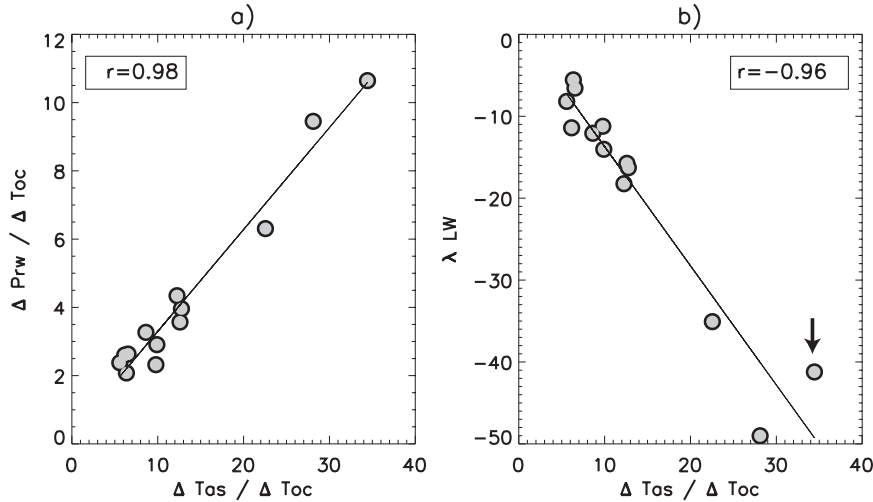


FIG. 5. (a) Scatterplot between $\Delta T_{as}/\Delta T_{oc}$ and $\Delta Prw/\Delta T_{oc}$ where Prw is the precipitable water (kg m^{-2}). (b) Scatterplot between $\Delta T_{as}/\Delta T_{oc}$ and λ_{LW} ($\text{W m}^{-2} \text{K}^{-1}$). The plain line is the regression line. The black arrow indicates the outlier shown in Fig. 7 and discussed in section 6. The correlations obtained when the three models with the most negative longwave feedback are excluded are (a) 0.83 and (b) -0.89 .

indicating that the negative shortwave component is dominant.

Since the contribution of cloud feedback to the spread of the longwave feedback parameter can be neglected, we turn to the role of temperature and water vapor feedbacks. In this context, Eq. (5) can be expressed as

$$\lambda_{LW} \approx \frac{\partial F}{\partial Prw} \frac{\Delta Prw}{\Delta T_{oc}} + \frac{\partial F}{\partial T_{as}} \frac{\Delta T_{as}}{\Delta T_{oc}}, \quad (6)$$

where Prw is the precipitable water. Figure 5a depicts the relation between $\Delta T_{as}/\Delta T_{oc}$ and $\Delta Prw/\Delta T_{oc}$. As expected given the link between temperature and humidity changes through the Clausius–Clapeyron relation, $\Delta T_{as}/\Delta T_{oc}$ and $\Delta Prw/\Delta T_{oc}$ are almost perfectly correlated. Figure 5b shows that the longwave feedback parameter λ_{LW} is highly correlated to the ratio $\Delta T_{as}/\Delta T_{oc}$ (and thus, given the previous result, to $\Delta Prw/\Delta T_{oc}$).

From Fig. 5, we can therefore write empirically that

$$\frac{\Delta Prw}{\Delta T_{oc}} \approx k \frac{\Delta T_{as}}{\Delta T_{oc}}, \quad \text{and} \quad (7)$$

$$\lambda_{LW} \approx a \frac{\Delta T_{as}}{\Delta T_{oc}}, \quad (8)$$

where a, k are constants that may be derived empirically. Note that from a statistical point of view, $\Delta T_{as}/\Delta T_{oc}$ or $\Delta Prw/\Delta T_{oc}$ can be used interchangeably in Eq. (8) given their near perfect correlation.

Based on Eqs. (7) and (6) we can write

$$\lambda_{LW} \approx k \frac{\partial F}{\partial Prw} \frac{\Delta T_{as}}{\Delta T_{oc}} + \frac{\partial F}{\partial T_{as}} \frac{\Delta T_{as}}{\Delta T_{oc}}. \quad (9)$$

Finally, equating Eqs. (8) and (9), we obtain

$$a \approx \left(\frac{\partial F}{\partial T_{as}} + k \frac{\partial F}{\partial Prw} \right). \quad (10)$$

The term a thus encapsulates both the effect of the water vapor and temperature feedback. Given Fig. 5b, a can be written as a constant, and the effect of the intermodel variations of $(\partial F/\partial T_{as}) + k(\partial F/\partial Prw)$ are negligible in the spread of λ_{LW} compared to those of $\Delta T_{as}/\Delta T_{oc}$. Therefore, we only have to study the spread of $\Delta T_{as}/\Delta T_{oc}$ to explain the spread in the longwave feedback parameter. However, it is still interesting to evaluate the two components of a , in order to disambiguate the respective roles of the water vapor and temperature feedbacks and better understand the physical mechanisms.

To do this, a one-dimensional radiative model is used. The model is the Column Radiative Model (CRM), which is a stand-alone version of the column radiation code employed by the NCAR Community Climate Model (Kiehl et al. 1996). To be more accurate in the evaluation of the temperature and water vapor feedbacks, the change of the vertical structure of atmospheric temperature and humidity are considered. Because the intermodel spread of a is negligible, the

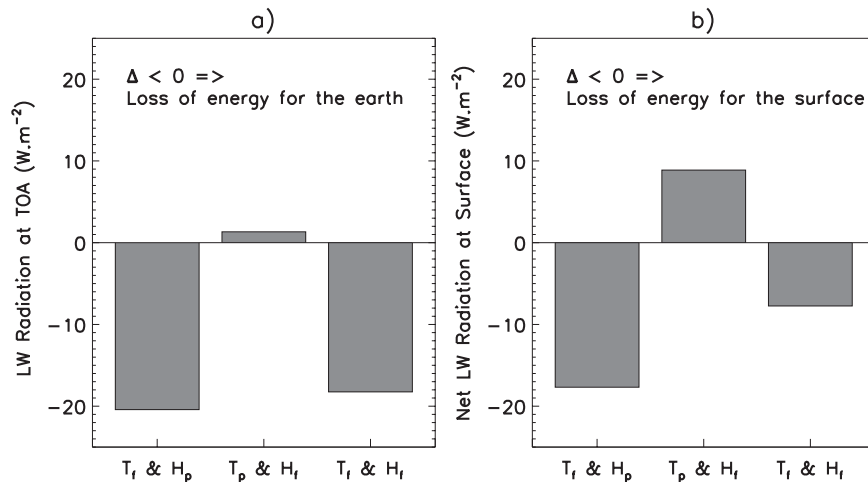


FIG. 6. Changes of (a) longwave radiation at the top of atmosphere and (b) net longwave radiation at surface simulated by a one-dimensional radiative model in clear-sky condition: (T_f and H_p) when the future (present) temperature (water vapor) profile is used, (T_p and H_f) when the present (future) temperature (water vapor) profile is used, and (T_f and H_f) when the future (future) temperature (water vapor) profile is used.

ensemble mean of the temperature and humidity profiles spatially averaged in the Arctic are computed in the present and future climates and the respective effects of the changes of the two profiles on longwave radiation at the TOA and on net longwave radiation at the surface are assessed in clear-sky conditions. The results are depicted in Fig. 6.

Figure 6 shows that changing the atmospheric humidity profile leads to a very small decrease of OLR compared to the very large increase of OLR that results from the modification of the temperature profile. At the surface, the change of temperature leads to a large loss of longwave radiation, while the change of humidity leads to a gain of energy. Note that the sum of the effects of the two perturbations is very similar to the effect of the two perturbations taken together, both for OLR and net radiation at the surface. The increase of humidity has thus a very weak direct effect on OLR, but has a positive effect on net longwave radiation at surface, and thus indirectly enhances the surface warming and the associated increase of OLR.

From this analysis we conclude that, even if the relative increase of water vapor is large in the Arctic, the associated greenhouse effect is relatively weak and cannot counteract the large increase of OLR that results from the increase of temperature. These results are consistent with spatial estimation of the feedbacks given by Soden et al. (2008), based on a different methodology. While water vapor feedback is known to play a key role in the tropics, this is not the case in the Arctic. This difference is probably linked to the extreme dryness of the atmo-

sphere in the Arctic, particularly in winter, and to the temperature inversion that occurs near the surface in the Arctic during winter and inhibits vertical heat and water transfer between the surface and the free troposphere. The changes of temperature and water vapor in the Arctic are thus trapped near the surface (not shown). Such an increase of water vapor near the surface is known to have only a weak effect on OLR (Held and Soden 2000). In fact, given the thermal inversion in the Arctic, the effect of a water vapor increase near the surface may even lead to an OLR increase and thus to a negative feedback as shown by Soden et al. (2008). Even if humidity also increases moderately above the inversion (not shown) where humidity exerts a positive longwave feedback, the overall effect of water vapor feedback in the Arctic remains small, as suggested by Fig. 6.

This weak water vapor feedback is a unique feature of Arctic climate change. In the tropics, a competition exists between the OLR increase that results from the increase of temperature and the OLR decrease due to the Clausius–Clapeyron-driven increase of water vapor. Such competition does not exist to nearly the same degree in the Arctic, as the countereffect of water vapor on the increase of OLR stemming from temperature change is weak. The Arctic climate, as simulated by the CMIP3 models, is thus characterized by a large capacity to radiate energy into space, given the relative weakness of the water vapor and longwave cloud feedbacks. This result explains why no unusual increase of heat content is seen in the Arctic, compared to other latitudes (Fig. 1), despite the powerful sea ice–snow albedo feedback.

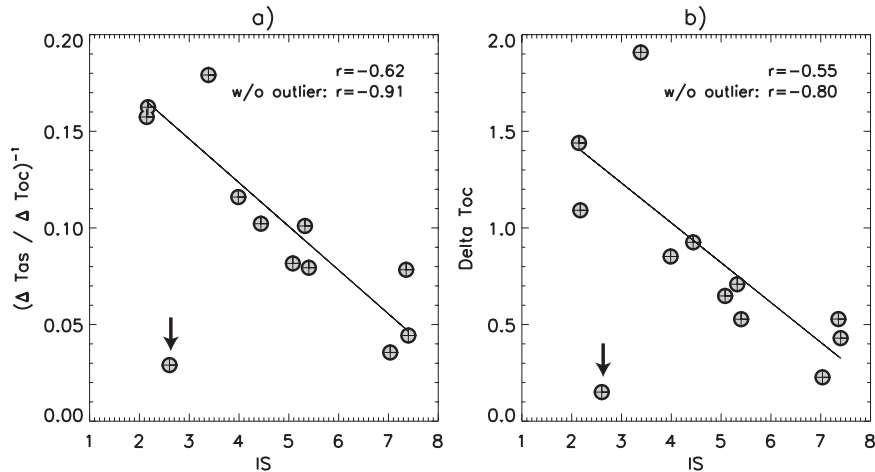


FIG. 7. Value of (a) $(\Delta T_{as}/\Delta T_{oc})^{-1}$ and (b) ΔT_{oc} in the CMIP3 models given the climatological strength of the inversion (IS, K) in the present climate (defined as the difference between $T_{a850hPa}$ and $T_{a1000hPa}$, from November to February). The inverse of the ratio $\Delta T_{as}/\Delta T_{oc}$ is used because its relation with the strength of the inversion is linear. The black arrow indicates the outlier.

6. Spread of the temperature feedback

From the previous section, it is clear that the temperature feedback factor $\Delta T_{as}/\Delta T_{oc}$ is a crucial contributor to the uncertainties of Arctic climate change. Different physical mechanisms may control its magnitude. One of them involves the inversion of the vertical temperature profile near the surface. Greater atmospheric stratification tends to trap the warming resulting from an increase of oceanic temperature and ice reduction near the surface, leading to larger values of the ratio $\Delta T_{as}/\Delta T_{oc}$. In this case, the climatological strength of the inversion in the present climate should be an important parameter. This hypothesis is tested in Fig. 7a. The strength of the inversion is computed as the climatological difference of atmospheric temperature between the 850- and 1000-hPa levels, from November to February, the main period when an inversion exists.

Figure 7a shows that, for a given ΔT_{oc} , ΔT_{as} is greater when the inversion is stronger in the present climate, consistent with the previous discussion. However, a clear outlier exists in this graph, corresponding to the model GISS-ER. This model has a large positive bias in areal coverage of sea ice, the greatest among the models studied here, especially in summer. It also has very thick ice in the present climate and its present-day seasonal cycle is very weak (Zhang and Walsh 2006). The sea ice cover simulated by this model hardly changes in the future climate and the sea ice thickness remains large compared to the other models, probably because it is difficult to trigger the sea ice albedo feedback given the climatological biases. Therefore, T_{oc} hardly increases at all in this model for a reason unrelated to longwave

feedback, hence the different behavior of this model. Note that this model also corresponds to the outliers seen in Figs. 4 and 5b and indicated with a black arrow, which reinforces our confidence in the idea that this model exhibits a different behavior than the other CMIP3 models, and should be thought of separately.

The value of $\Delta T_{as}/\Delta T_{oc}$ is thus strongly linked to a simulated characteristic of the present climate, the strength of the inversion. Since $\Delta T_{as}/\Delta T_{oc}$ explains a large part of the variations in λ_{LW} , and λ_{LW} explains a large part of ΔT_{oc} , as shown in the previous sections, a strong link between ΔT_{oc} and the strength of the inversion in the present climate is found when the outlier is removed (Fig. 7b, the correlation is -0.80), as expected.

7. Implications

The previous result is significant because the climatological strength of the inversion in the present climate is a testable feature we can use to derive information about the realism of simulated temperature feedback in the CMIP3 models. However, climatological observations of the vertical profile of temperature are too sparse in our study area and especially over the Arctic Ocean, and therefore we have to rely on reanalyses. Graversen et al. (2008) compared atmospheric temperature from reanalyses to available soundings in the Arctic and showed that the vertical structure of temperature in 40-yr European Centre for Medium-Range Weather Forecasts (ECMWF) Re-Analysis (ERA-40) and National Centers for Environmental Prediction (NCEP) reanalyses is realistic (supplementary Fig. 1) even if there is a small

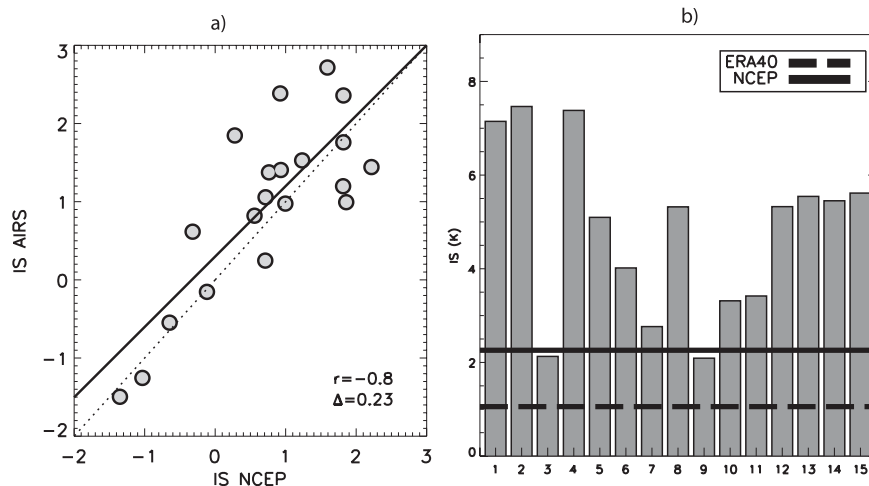


FIG. 8. (a) Comparison of the strength of the inversion (K) in NCEP reanalysis and in AIRS satellite data from November 2003 to February 2008. Each point is a month of the November–February season. Here Δ is the mean difference between AIRS and NCEP climatologies. (b) Climatological strength of the inversion (IS, K) in the 1960–99 period as simulated by the CMIP3 models and given by the ERA-40 and NCEP reanalysis products. All the available models are used: 1) CCCma CGCM3.1; 2) CCCma CGCM3.1 T63; 3) CNRM-CM3; 4) CSIRO Mk3.0; 5) GFDL CM2.0; 6) GFDL CM2.1; 7) GISS-ER; 8) Institute of Numerical Mathematics Coupled Model, version 3.0 (INM-CM3.0); 9) IPSL CM4; 10) MIROC3.2(medres); 11) Max Planck Institute (MPI) ECHAM5; 12) MRI CGCM2.3.2a; 13) NCAR Community Climate System Model, version 3.0 (CCSM3.0); 14) NCAR PCM1; 15) UKMO Hadley Centre Global Environmental Model version 1 (HadGEM1).

tendency to underestimate the difference of temperature between $T_{a_{850\text{hPa}}}$ and $T_{a_{1000\text{hPa}}}$ (around 0.5° for NCEP). Note that the use of atmospheric reanalyses by Graversen et al. (2008) to study trends in atmospheric temperature profile in the Arctic has been challenged by Thorne (2008), Grant et al. (2008), and Bitz and Fu (2008), but the overall ability of the reanalyses to capture the climatological vertical temperature structure of temperature is not in question in these studies.

As available soundings are mainly over land areas, the conclusion of Graversen et al. (2008) regarding the realism of the climatological vertical temperature structure in reanalyses may not stand in the Arctic Ocean region, where the inversion strength is generally smaller than over surrounding land areas. We therefore also compared the value of the strength of inversion in the NCEP reanalysis to *Aqua* Atmospheric Infrared Sounder (AIRS) satellite measurements (Olsen 2007; Divakarla et al. 2006) from November to February, on the overlapping period between the two datasets (November 2003 to February 2008). Even if the month-to-month variations of the inversion in the two datasets do not perfectly match, the climatological values are very similar (Fig. 8a). Pending more in situ observations over the Arctic Ocean itself, those two lines of evidence reinforce our confidence in the ability of the reanalyses to capture the long-term climatological value of the inversion.

Figure 8b shows the value of the inversion strength for the ERA-40 and NCEP reanalysis and the CMIP3 models for the 1960–99 period. As a group, the CMIP3 models have a cold bias both at 1000 and 850 hPa, but the bias is greater at 1000 hPa (not shown). Therefore, compared to the ERA-40 or NCEP reanalysis, almost all the models overestimate the value of the inversion, many of them by more than a factor of 2. Because the possible underestimation of the strength of the inversion in the ERA-40 and NCEP reanalyses is small, we conclude it is likely that most of the CMIP3 models overestimate the strength of the inversion, sometimes greatly. The models are therefore likely to overestimate the negative temperature feedback, and consequently the negative longwave feedback, leading to an underestimation of the change of oceanic temperature in response to external forcing.

In this study, we focused on the change of oceanic temperature because it is a key variable to understand the mechanisms of Arctic climate change, but it may not be the main variable of interest from a practical point of view. However, there is a strong link between ΔT_{oc} and the change in sea ice cover, a variable of widespread interest, as shown in Fig. 9b. A relation also exists between ΔT_{as} and ΔT_{oc} (Fig. 9a, correlation of 0.71). We saw previously that, when normalized by ΔT_{oc} , a larger ΔT_{as} is linked to a larger negative feedback and hence a

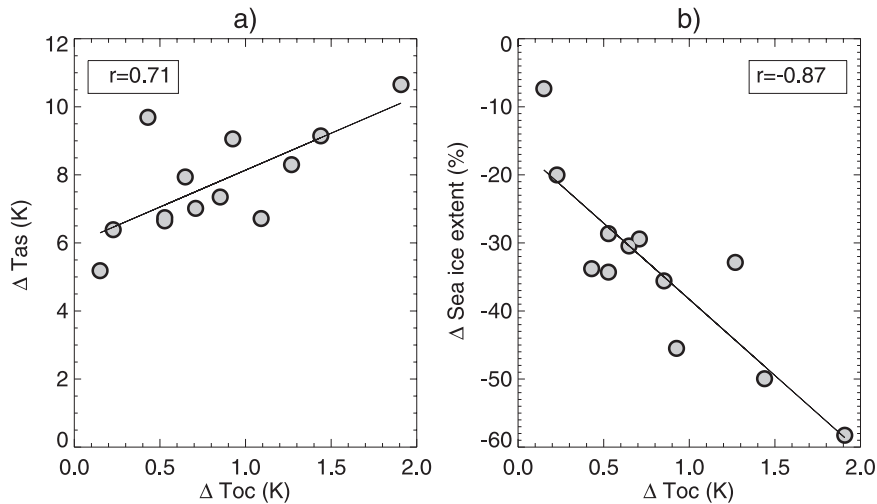


FIG. 9. Scatterplot between (a) ΔT_{oc} and ΔT_{as} and between (b) ΔT_{oc} and the relative change of sea ice extent.

smaller increase in ΔT_{oc} . This apparent contradiction highlights the importance of normalization by ΔT_{oc} to elucidate the feedback processes. Ultimately, the smaller increase of T_{oc} associated with a stronger negative feedback leads to a smaller change in sea ice and reduces the (nonnormalized) surface temperature change.

8. Summary and concluding remarks

In this paper, we use a specific feedback analysis framework to study the uncertainties of Arctic climate change. An ensemble of climate models from the CMIP3 archive is studied. We focus on the analysis of oceanic temperature change, as this variable is found to play a central role in the mechanisms of Arctic climate change. The analysis shows that a large part of the spread of oceanic temperature change is explained by the longwave feedback parameter. Surprisingly, the role of the shortwave feedback is secondary. As stated by Serreze and Francis (2006), the Arctic warming depends on how much energy gained during summer thanks to the sea ice albedo feedback and stored in the ocean may be carried through winter. In this paper, we show that it is not the degree to which the models gain energy during summer, but rather their capacity to radiate the energy out during winter, that primarily explains the large spread of the CMIP3 model results.

In the Arctic, the negative longwave feedback is particularly strong because of weak positive longwave cloud cover and water vapor feedbacks. Generally, given the strong link between atmospheric temperature and humidity changes, a competition exists between the increase of the radiative cooling directly caused by tem-

perature change and the increase of the greenhouse effect caused by humidity change, which is indirectly linked to temperature change. In the Arctic, the effect of temperature change is overwhelming as the additional greenhouse effect due to the increase of humidity is weak. The physical explanation is that the climatological inversion of the atmospheric temperature near the surface during winter acts to trap the increase of humidity near the surface, where it leads to an increase rather than a decrease of OLR (Soden et al. 2008). It is also shown in the paper that the cloud feedback plays little role in the spread of the longwave feedback parameter.

During summer, the sea ice albedo feedback leads to a high level of positive feedback in the Arctic: the sea ice cover decreases and energy is stored in the ocean. But during winter, the decrease of sea ice cover has an opposite effect: because of the insulation effect of sea ice, its disappearance leads to large transfer of energy from the ocean to the atmosphere. This energy is ultimately very efficiently radiated to space because of weak longwave cloud and water vapor feedbacks. The large Arctic amplification of surface temperature is mainly a by-product of this large seasonal redistribution of energy. Because of the high level of negative feedback in winter in the Arctic, the positive oceanic temperature anomalies generated during summer are damped very efficiently, explaining why no amplification of heat content change is found in the Arctic, despite the powerful positive sea ice–snow albedo feedback.

We also show that the climatological strength of the inversion plays a major role in the uncertainties of Arctic climate change, through the modulation of the temperature feedback. Indeed, a strong inversion leads

to a large increase of surface temperature in response to a given increase of oceanic temperature and thus to a large negative longwave feedback.

As most of the CMIP3 models are likely to largely overestimate the strength of the inversion, they may overestimate the negative longwave feedback and the CMIP3 models may, as a group, underestimate future Arctic climate change. As a matter of fact, the two models that exhibit the stronger response in the Arctic are the ones with the most realistic representation of the strength of the inversion in the present climate.

In spite of the small number of models studied, there are clearly visible relationships among the various physical parameters studied, consistent with the reasonable levels of statistical significance of the correlations among them. We therefore conclude our main results are unlikely to be significantly different if we had more models to analyze. In conclusion, there are good reasons to think the negative longwave feedback is too strong in most current climate models and, consequently, that simulated Arctic climate changes may have an unrealistically small magnitude. This conclusion raises the question of whether the large underestimation of the declining trend in sea ice extent simulated by most CMIP3 models noted by Stroeve et al. (2007) may be related to the overestimation of the negative feedback described in this paper. We tested this hypothesis and found it is not case. Indeed, there is only a weak anticorrelation (-0.33) between the sum of the feedback parameters estimated in this study and the trends in September sea ice extent in the 1979–2007 period. Different processes therefore govern transient and near-equilibrium climate change in the Arctic. A future study will address this issue.

Acknowledgments. The authors are supported by NSF ARC-0714083. Opinions, findings, conclusions, or recommendations expressed here are those of the authors and do not necessarily reflect NSF views. We acknowledge the modeling groups, the Program for Climate Model Diagnosis and Intercomparison (PCMDI) and the WCRP's Working Group on Coupled Modelling (WGCM) for their roles in making available the WCRP CMIP3 multimodel dataset. Support of this dataset is provided by the Office of Science, U.S. Department of Energy. ERA-40 data used in this study have been obtained from the ECMWF data server.

REFERENCES

- Bitz, C. M., and Q. Fu, 2008: Arctic warming aloft is data set dependent. *Nature*, **455**, E3–E4.
- Bony, S., and Coauthors, 2006: How well do we understand and evaluate climate change feedback processes? *J. Climate*, **19**, 3445–3482.
- Budyko, M. I., 1969: The effect of solar radiation variations on the climate of the earth. *Tellus*, **21**, 611–619.
- Cai, M., 2006: Dynamical greenhouse-plus feedback and polar warming amplification. Part I: A dry radiative-transportive climate model. *Climate Dyn.*, **26**, 661–675.
- Curry, J. A., J. L. Schramm, and E. E. Ebert, 1995: Sea ice-albedo climate feedback mechanism. *J. Climate*, **8**, 240–247.
- de Boyer Montégut, C., G. Madec, A. S. Fischer, A. Lazar, and D. Iudicone, 2004: Mixed layer depth over the global ocean: An examination of profile data and a profile-based climatology. *J. Geophys. Res.*, **109**, C12003, doi:10.1029/2004JC002378.
- Divakarla, M. G., C. D. Barnet, M. D. Goldberg, L. M. McMillin, E. S. Maddy, W. W. Wolf, L. Zhou, and X. Liu, 2006: Validation of Atmospheric Infrared Sounder temperature and water vapor retrievals with matched radiosonde measurements and forecasts. *J. Geophys. Res.*, **111**, D09S15, doi:10.1029/2005JD006116.
- Grant, A. N., S. Brönnimann, and L. Haimberger, 2008: Recent Arctic warming vertical structure contested. *Nature*, **455**, E2–E3.
- Graversen, R. G., T. Mauritsen, M. Tjernström, E. Källén, and G. Svensson, 2008: Vertical structure of recent Arctic warming. *Nature*, **451**, 53–56.
- Hall, A., 2004: The role of surface albedo feedback in climate. *J. Climate*, **17**, 1550–1568.
- Hegerl, G. C., and Coauthors, 2007: Understanding and attributing climate change. *Climate Change 2007: The Physical Science Basis*, S. Solomon et al., Eds., Cambridge University Press, 663–745.
- Held, I. M., and B. J. Soden, 2000: Water vapor feedback and global warming. *Annu. Rev. Energy Environ.*, **25**, 441–475.
- Holland, M. M., and C. M. Bitz, 2003: Polar amplification of climate change in coupled models. *Climate Dyn.*, **21**, 221–232.
- , —, and B. Tremblay, 2006: Future abrupt reductions in the summer Arctic sea ice. *Geophys. Res. Lett.*, **33**, L23503, doi:10.1029/2006GL028024.
- Kiehl, J. T., J. J. Hack, G. B. Bonana, B. A. Boville, B. P. Briegleb, D. L. Williamson, and P. J. Rasch, 1996: Description of the NCAR Community Climate Model (CCM3). NCAR Tech. Note NCAR/TN-420+STR, 152 pp.
- Manabe, S., and R. J. Stouffer, 1980: Sensitivity of a global climate model to an increase of CO₂ concentration in the atmosphere. *J. Geophys. Res.*, **85**, 5529–5554.
- Meehl, G. A., and Coauthors, 2007a: Global climate projections. *Climate Change 2007: The Physical Science Basis*, S. Solomon et al., Eds., Cambridge University Press, 747–845.
- , C. Covey, T. Delworth, M. Latif, B. McAvaney, J. F. B. Mitchell, R. J. Stouffer, and K. E. Taylor, 2007b: The WCRP CMIP3 multimodel dataset: A new era in climate change research. *Bull. Amer. Meteor. Soc.*, **88**, 1383–1394.
- Olsen, E. T., Ed., 2007: AIRS/AMSU/HSB version 5 data release user guide. NASA-JPL Tech. Rep., 68 pp. [Available online at http://disc.sci.gsfc.nasa.gov/AIRS/documentation/v5_docs/AIRS_V5_Release_User_Docs/V5_Data_Release_UG.pdf.]
- Robock, A., 1985: An updated climate feedback diagram. *Bull. Amer. Meteor. Soc.*, **66**, 786–787.
- Sellers, W. D., 1969: A global climatic model based on the energy balance of the earth system. *J. Appl. Meteor.*, **8**, 392–400.
- Serreze, M. C., and J. A. Francis, 2006: The Arctic amplification debate. *Climatic Change*, **76**, 241–264.
- , M. M. Holland, and J. Stroeve, 2007: Perspectives on the Arctic's shrinking sea-ice. *Science*, **315**, 1533–1536, doi:10.1126/science.1139426.
- Soden, B. J., I. M. Held, R. Colman, K. M. Shell, J. T. Kiehl, and C. A. Shields, 2008: Quantifying climate feedbacks using radiative kernels. *J. Climate*, **21**, 3504–3520.

- Solomon, S., D. Qin, M. Manning, M. Marquis, K. Averyt, M. M. B. Tignor, H. L. Miller Jr., and Z. Chen, Eds., 2007: *Climate Change 2007: The Physical Science Basis*. Cambridge University Press, 996 pp.
- Stroeve, J., M. M. Holland, W. Meier, T. Scambos, and M. Serreze, 2007: Arctic sea ice decline: Faster than forecast. *Geophys. Res. Lett.*, **34**, L09501, doi:10.1029/2007GL029703.
- Tebaldi, C., and R. Knutti, 2007: The use of the multi-model ensemble in probabilistic climate projections. *Philos. Trans. Roy. Soc. London*, **A365**, 2053–2075, doi:10.1098/rsta.2007.2076.
- Thorne, P. W., 2008: Arctic tropospheric warming amplification? *Nature*, **455**, E1–E2.
- Wetherald, R. T., and S. Manabe, 1988: Cloud feedback processes in a general circulation model. *J. Atmos. Sci.*, **45**, 1397–1415.
- Winton, M., 2006: Amplified Arctic climate change: What does surface albedo feedback have to do with it? *Geophys. Res. Lett.*, **33**, L03701, doi:10.1029/2005GL025244.
- Zhang, J., R. Lindsay, M. Steele, and A. Schweiger, 2008: What drove the dramatic retreat of Arctic sea ice during summer 2007? *Geophys. Res. Lett.*, **35**, L11505, doi:10.1029/2008GL034005.
- Zhang, X., and J. E. Walsh, 2006: Toward a seasonally ice-covered Arctic Ocean: Scenarios from the IPCC AR4 model simulations. *J. Climate*, **19**, 1730–1747.